Optica Applicata, Vol. XLVI, No. 1, 2016
DOI: 10.5277/oa160101

Astigmatic transformation of Bessel beams in a uniaxial crystal

SVETLANA N. KHONINA[1, 2], VYACHESLAV D. PARANIN[2],
ANDREY V. USTINOV[1], ANDREY P. KRASNOV[2]

[1]Image Processing Systems Institute of the RAS,
Molodogvardeyskaya 151, Samara, 443001, Russia

[2]Samara State Aerospace University,
Moskovskoye Shosse 34, Samara, 443086, Russia

We investigate theoretically and experimentally the astigmatic transformations of Bessel beams at propagation perpendicularly to the *c*-axis of a uniaxial crystal. The analogy between this transformation and the astigmatic distortion of the plane wave by an inclined axicon is analytically shown. The influence of the polarization direction of radiation relative to the *c*-axis of a crystal on electric field components of the ordinary and the extraordinary beams is investigated.

Keywords: Bessel beams, axicon, astigmatic transformations, uniaxial crystal, polarization.

1. Introduction

Optical devices that make it possible to transform some properties of electromagnetic radiation into other are subject of increasing interest and find more practical applications. Mode transformations (from the fundamental mode into higher-order distributions) and polarization transformations (from homogeneous linear polarization into more complex types) are the most often required ones. Anisotropic crystals are tools of such transformations. Nonparaxial propagation of laser modes in a medium with strong anisotropy results in complex polarization-mode transformations [1–12].

In particular, in case of propagation along the crystal *c*-axis, the spin angular momentum that has a circularly polarized beam is transformed into orbital angular momentum. It was shown in [4–7] that in propagating along the crystal *c*-axis nonparaxial Bessel beams periodically change their intensity, which corresponds to the transformation into a higher-order beam.

In [2, 3, 9–12] propagation of various types of laser beams perpendicular to the crystal *c*-axis was analyzed. However, the most interesting transformations were observed in case of Bessel beams [2, 3, 9] as in this case the visible astigmatic distortion of the beam circular structure takes place. Similar distortion can be observed in case of the oblique plane wave incidence on axicons [13–16] as well as in case of using

a cylindrical lens [17]. This analogy was noted in [3], however, the effect was not analytically proven.

This paper presents a detailed theoretical, numerical and experimental analysis of the effect of astigmatic transformation of Bessel beams propagating perpendicular to the crystal *c*-axis. The analogy between the astigmatic transformations produced by an anisotropic medium and the oblique incidence of radiation on an axicon is shown analytically. The influence of the relative position of the radiation polarization plane and the crystal *c*-axis on intensity distributions formed in various vector components of the ordinary and the extraordinary beams is investigated.

2. Theoretical analysis

Diffraction patterns in laser beam propagation along the crystal *c*-axis and perpendicular to it look different. The degree of the difference depends on the type of beam as well. For example, comparative analysis of Bessel and Gauss–Laguerre mode laser beams in a uniaxial crystal in various directions was carried out in [7, 8].

It was shown that in case of propagation along the crystal *c*-axis, laser radiation with high numerical aperture is subject to periodic variation of intensity caused by polarization transformation [5, 7]. The fact of partial energy transfer into orthogonal components in case of sharp focusing in isotropic and anisotropic media was also discussed in [1, 4, 8, 18, 19].

Let us analyze the situation when the electromagnetic wave propagates perpendicular to the crystal *c*-axis (Fig. 1) in more detail.

Beam propagation in a uniaxial crystal can be described on the basis of expansion in plane waves [20]:

$$\begin{bmatrix}\mathbf{E}(u,v,z)\\ \mathbf{H}(u,v,z)\end{bmatrix} = \iint\limits_{\alpha^2+\beta^2\le 1} \left\{ c_1(\alpha,\beta)\begin{bmatrix}\mathbf{e}_1(\alpha,\beta)\\ \mathbf{h}_1(\alpha,\beta)\end{bmatrix}\exp[ik\gamma_1(\alpha,\beta)z] + \right.$$

$$\left. + c_2(\alpha,\beta)\begin{bmatrix}\mathbf{e}_2(\alpha,\beta)\\ \mathbf{h}_2(\alpha,\beta)\end{bmatrix}\exp[ik\gamma_2(\alpha,\beta)z]\right\}\exp[ik(\alpha u+\beta v)]\,\mathrm{d}\alpha\,\mathrm{d}\beta \tag{1}$$

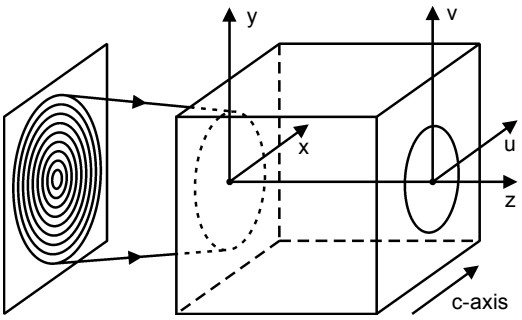

Fig. 1. Explanatory scheme.

where α and β are spatial frequencies, λ is the length of wave radiation in vacuum, $k = 2\pi/\lambda$ is the wave number. The expansion coefficients in (1) have the form:

$$c_1(\alpha, \beta) = \Delta^{-1}[S_x(\alpha, \beta)e_{2y}(\alpha, \beta) - S_y(\alpha, \beta)e_{2x}(\alpha, \beta)] \tag{2a}$$

$$c_2(\alpha, \beta) = \Delta^{-1}[S_y(\alpha, \beta)e_{1x}(\alpha, \beta) - S_x(\alpha, \beta)e_{1y}(\alpha, \beta)] \tag{2b}$$

where $\Delta = e_{1x}(\alpha, \beta)e_{2y}(\alpha, \beta) - e_{1y}(\alpha, \beta)e_{2x}(\alpha, \beta)$.

The spatial spectrum is calculated only for transverse components of the electrical component of the incident wave,

$$S_{x,y}(\alpha, \beta) = \frac{1}{\lambda^2}\iint_{\Omega} E_{x,y}(x, y, 0)\exp[-ik(\alpha x + \beta y)]\,\mathrm{d}x\,\mathrm{d}y \tag{3}$$

For a uniaxial crystal, the *c*-axis of which is perpendicular to the axis of the light beam propagation and directed along the coordinate axis *x*, the eigenvectors $\mathbf{e}_j(\alpha, \beta)$, $\mathbf{h}_j(\alpha, \beta)$ and eigenvalues $\gamma_j(\alpha, \beta)$ have the form:

$$\begin{bmatrix} e_{1x} \\ e_{1y} \\ e_{1z} \\ h_{1x} \\ h_{1y} \\ h_{1z} \end{bmatrix} = \begin{bmatrix} \alpha^2 - \varepsilon_1\mu \\ \alpha\beta \\ \alpha\gamma_1(\alpha, \beta) \\ 0 \\ -\varepsilon_1\gamma_1(\alpha, \beta) \\ \beta\varepsilon_1 \end{bmatrix} \tag{4a}$$

$$\begin{bmatrix} e_{2x} \\ e_{2y} \\ e_{2z} \\ h_{2x} \\ h_{2y} \\ h_{2z} \end{bmatrix} = \frac{1}{\mu\gamma_2(\alpha, \beta)} \begin{bmatrix} 0 \\ \mu\gamma_2(\alpha, \beta) \\ -\mu\beta \\ \alpha^2 - \mu\varepsilon_1 \\ \alpha\beta \\ \alpha\gamma_2(\alpha, \beta) \end{bmatrix} \tag{4b}$$

$$\gamma_1(\alpha, \beta) = \sqrt{\varepsilon_2\mu - \frac{\varepsilon_2}{\varepsilon_1}\alpha^2 - \beta^2} \tag{5a}$$

$$\gamma_2(\alpha, \beta) = \sqrt{\varepsilon_1\mu - \alpha^2 - \beta^2} \tag{5b}$$

where ε_1 and ε_2 are ordinary and extraordinary permittivities of a uniaxial crystal, μ is the permeability.

Since only the electrical component of the electromagnetic wave is registered, we shall write its propagation for the case when the crystal *c*-axis is directed along the coordinate axis *x* (in the absence of extraneous charges $\mu = 1$):

$$\begin{aligned}\mathbf{E}(u, v, z) = & \iint\limits_{\alpha^2+\beta^2\le 1} \frac{S_x(\alpha, \beta)}{\varepsilon_1\mu - \alpha^2} \begin{bmatrix} \varepsilon_1\mu - \alpha^2 \\ \alpha\beta \\ \alpha\gamma_1(\alpha, \beta) \end{bmatrix} \times \\ & \times \exp\left\{ik\left[\alpha u + \beta v + \gamma_1(\alpha, \beta) z\right]\right\} \mathrm{d}\alpha\,\mathrm{d}\beta + \\ & + \iint\limits_{\alpha^2+\beta^2\le 1} \frac{S_y(\alpha, \beta)(\alpha^2 - \varepsilon_1\mu) - S_x(\alpha, \beta)\alpha\beta}{(\varepsilon_1\mu - \alpha^2)\mu\gamma_2(\alpha, \beta)} \begin{bmatrix} 0 \\ \mu\gamma_2(\alpha, \beta) \\ -\mu\beta \end{bmatrix} \times \\ & \times \exp\left\{ik\left[\alpha u + \beta v + \gamma_2(\alpha, \beta) z\right]\right\} \mathrm{d}\alpha\,\mathrm{d}\beta \end{aligned} \tag{6}$$

In Eq. (6) the first integral corresponds to an extraordinary beam and the second one to an ordinary beam. As follows from (6), total distribution depends on the polarization of the incident beam significantly.

In [7, 8] it was shown that the energy of the longitudinal component is insignificant as compared to the contribution of the transverse components even for high numerical apertures of the incident field. This is due to high values of crystal refractive index (usually more than 2) as compared to free space from which the radiation is emitted. In this connection let us examine in more detail only the transverse components of ordinary (*o*) and extraordinary (*e*) beams:

$$E_x^o(u, v, z) = 0 \tag{7a}$$

$$\begin{aligned} E_y^o(u, v, z) = & \iint\limits_{\alpha^2+\beta^2\le 1} \frac{S_y(\alpha, \beta)(\alpha^2 - \varepsilon_1\mu) - S_x(\alpha, \beta)\alpha\beta}{\varepsilon_1\mu - \alpha^2} \times \\ & \times \exp\left\{ik\left[\alpha u + \beta v + \gamma_2(\alpha, \beta) z\right]\right\} \mathrm{d}\alpha\,\mathrm{d}\beta \end{aligned} \tag{7b}$$

$$E_x^e(u, v, z) = \iint\limits_{\alpha^2+\beta^2\le 1} S_x(\alpha, \beta) \exp\left\{ik\left[\alpha u + \beta v + \gamma_1(\alpha, \beta) z\right]\right\} \mathrm{d}\alpha\,\mathrm{d}\beta \tag{7c}$$

$$E_y^e(u, v, z) = \iint\limits_{\alpha^2+\beta^2 \le 1} \frac{S_x(\alpha, \beta)\alpha\beta}{\varepsilon_1\mu - \alpha^2} \exp\left\{ik\left[\alpha u + \beta v + \gamma_1(\alpha, \beta)z\right]\right\} \mathrm{d}\alpha\,\mathrm{d}\beta \qquad (7\mathrm{d})$$

It follows from (7) that the x-component is absent in an ordinary beam at the output of the crystal, the c-axis of which is oriented along the coordinate axis x. Moreover, if the beam incident on the crystal has polarization perpendicular to the crystal c-axis, an extraordinary beam will be absent at the crystal output altogether. An ordinary beam in this case will propagate in the same way as in an isotropic medium

$$E_y^o(u, v, z) = -\iint\limits_{\alpha^2+\beta^2 \le 1} S_y(\alpha, \beta) \exp\left\{ik\left[\alpha u + \beta v + z\sqrt{\varepsilon_1\mu - \alpha^2 - \beta^2}\right]\right\} \mathrm{d}\alpha\,\mathrm{d}\beta \qquad (8)$$

If the polarization of the beam incident on the crystal is parallel to the crystal c-axis, radial symmetry at the crystal output will be broken:

$$E_x^e(u, v, z) = \iint\limits_{\alpha^2+\beta^2 \le 1} S_x(\alpha, \beta) \exp\left\{ik\left[\alpha u + \beta v + z\sqrt{\varepsilon_2\mu - \frac{\varepsilon_2}{\varepsilon_1}\alpha^2 - \beta^2}\right]\right\} \mathrm{d}\alpha\,\mathrm{d}\beta \qquad (9\mathrm{a})$$

$$E_y^o(u, v, z) + E_y^e(u, v, z) = \iint\limits_{\alpha^2+\beta^2 \le 1} \frac{S_x(\alpha, \beta)\alpha\beta}{\varepsilon_1\mu - \alpha^2} \exp[ik(\alpha u + \beta v)] \times$$
$$\times \left\{\exp\left[ikz\sqrt{\varepsilon_2\mu - \frac{\varepsilon_2}{\varepsilon_1}\alpha^2 - \beta^2}\right] - \exp\left[ikz\sqrt{\varepsilon_1\mu - \alpha^2 - \beta^2}\right]\right\} \mathrm{d}\alpha\,\mathrm{d}\beta \qquad (9\mathrm{b})$$

It follows from the expression (9b) that the y-component of the incident wave (perpendicular to the crystal c-axis) is subject to periodic changes connected with the multiplier $\exp\left(ikz\sqrt{\varepsilon_2\mu - \frac{\varepsilon_2}{\varepsilon_1}\alpha^2 - \beta^2}\right) - \exp\left(ikz\sqrt{\varepsilon_1\mu - \alpha^2 - \beta^2}\right)$. However, this effect is practically unnoticeable against the background of a more powerful x-component.

The component of the extraordinary beam parallel to the crystal c-axis is of greater interest. In accordance with the form $\gamma_1(\alpha, \beta)$ in Eq. (5a), it is this part of the electric field that is subject to astigmatic changes. We shall demonstrate it analytically taking a Bessel beam as an example.

For Bessel beams the spatial spectrum is concentrated in a narrow ring, the radius of which is related to the numerical aperture of the beam. For theoretical calculations it can be approximately described by the following formula: $S_{x,y}(\alpha, \beta) = c_{x,y}\delta(\alpha^2+\beta^2=\sigma_0^2)$, where $c_{x,y}$ are polarization coefficients, $\delta(\cdot)$ is the delta-function, σ_0 is the numerical aperture of the beam incident on the crystal.

Let us rewrite (9a) in polar form:

$$E_x^e(\rho,\,\psi,\,z) \;=\; c_x \iint\limits_{\sigma^2 \le 1} \delta(\sigma-\sigma_0)\exp\left\{ ik\left[\rho\sigma\cos(\theta-\psi) + \right.\right.$$

$$\left.\left. +\; z\sqrt{\varepsilon_2\mu - \frac{\varepsilon_2}{\varepsilon_1}[\sigma\cos(\theta)]^2 - [\sigma\sin(\theta)]^2}\right]\right\}\sigma\,\mathrm{d}\sigma\,\mathrm{d}\theta \;=$$

$$= c_x\sigma_0 \int\limits_0^{2\pi} \exp\left\{ ik\left[\rho\sigma_0\cos(\theta-\psi) + z\sqrt{\varepsilon_2\mu - \sigma_0^2\left(\frac{\varepsilon_2}{\varepsilon_1}\cos^2(\theta) + \sin^2(\theta)\right)}\right]\right\}\mathrm{d}\theta \tag{10}$$

To make an approximate calculation of the integral in (10), we shall make the following transformations. Let us consider the permittivities to differ insignificantly (not more than by 10%) and take into account the relationship $\varepsilon_1 > \varepsilon_2$ that takes place in the crystal under consideration. In this case we use the representation $\varepsilon_2/\varepsilon_1 = 1 - \Delta$ and root expansion into a series:

$$\sqrt{\varepsilon_2\mu - \sigma_0^2\left(\frac{\varepsilon_2}{\varepsilon_1}\cos^2(\theta) + \sin^2(\theta)\right)} \;=\; \sqrt{\varepsilon_2\mu - \sigma_0^2 + \sigma_0^2\Delta\cos^2(\theta)} \;\approx$$

$$\approx \sqrt{\varepsilon_2\mu - \sigma_0^2} \;+\; \frac{\sigma_0^2\Delta\cos^2(\theta)}{2\sqrt{\varepsilon_2\mu - \sigma_0^2}} \tag{11}$$

Applying this approximation to (10), we get

$$E_x^e(\rho,\,\psi,\,z) \;=\; c_x\sigma_0\exp\left(ikz\sqrt{\varepsilon_2\mu - \sigma_0^2}\right) \times$$

$$\times \int\limits_0^{2\pi} \exp\left\{ ik\left[\rho\sigma_0\cos(\theta-\psi) + \frac{z\sigma_0^2\Delta\cos^2(\theta)}{2\sqrt{\varepsilon_2\mu - \sigma_0^2}}\right]\right\}\mathrm{d}\theta \tag{12}$$

Using the equation $\cos^2(\theta) = [1 + \cos(2\theta)]/2$ and expansion [21]

$$\exp[ix\cos(t)] \;=\; \sum_{m\,=\,-\infty}^{\infty} i^m\exp(imt)J_m(x) \tag{13}$$

we can rewrite Eq. (12) in the following form:

$$E_x^e(\rho,\,\psi,\,z) \;=\; c_x\sigma_0\exp\left[ikz\left(\sqrt{\varepsilon_2\mu-\sigma_0^2}\;+\frac{\sigma_0^2\Delta}{4\sqrt{\varepsilon_2\mu-\sigma_0^2}}\right)\right]\times$$

$$\times\int_0^{2\pi}\exp[ik\rho\sigma_0\cos(\theta-\psi)]\sum_{m=-\infty}^{\infty}i^m\exp(2im\theta)J_m\left(\frac{kz\sigma_0^2\Delta}{4\sqrt{\varepsilon_2\mu-\sigma_0^2}}\right)\mathrm{d}\theta \tag{14}$$

Using in (14) the standard integral [22]:

$$\int_0^{2\pi}\exp[ix\cos(\tau)+in\tau]\,\mathrm{d}\tau \;=\; 2\pi(-i)^nJ_n(x) \tag{15}$$

we get

$$E_x^e(\rho,\,\psi,\,z) \;=\; 2\pi c_x\sigma_0\exp\left[ikz\left(\sqrt{\varepsilon_2\mu-\sigma_0^2}\;+\frac{\sigma_0^2\Delta}{4\sqrt{\varepsilon_2\mu-\sigma_0^2}}\right)\right]\times$$

$$\times\sum_{m=-\infty}^{\infty}(-i)^m\exp(2im\psi)J_m\left(\frac{kz\sigma_0^2\Delta}{4\sqrt{\varepsilon_2\mu-\sigma_0^2}}\right)J_{2m}(k\sigma_0\rho) \tag{16}$$

The intensity for the complex field (16) is written as follows:

$$I_x^e(\rho,\,\psi,\,z) \;=\; 4\pi^2\sigma_0^2\left|c_x\sum_{m=-\infty}^{\infty}(-i)^m\exp(2im\psi)J_m\left(\frac{kz\sigma_0^2\Delta}{4\sqrt{\varepsilon_2\mu-\sigma_0^2}}\right)J_{2m}(k\sigma_0\rho)\right|^2 \tag{17}$$

Taking (17) to be not very distant from the optical axis ($\rho\to 0$) in the infinite sum, we can restrict ourselves to three summands corresponding to $m = 0, \pm 1$:

$$J_0\left(\frac{kz\sigma_0^2\Delta}{4\sqrt{\varepsilon_2\mu-\sigma_0^2}}\right)J_0(k\sigma_0\rho)-2iJ_1\left(\frac{kz\sigma_0^2\Delta}{4\sqrt{\varepsilon_2\mu-\sigma_0^2}}\right)J_2(k\sigma_0\rho)\cos(2\psi)$$

Thus, we finally obtain

$$I_x^e(\rho,\ \psi,\ z) \approx 4\pi^2\sigma_0^2|c_x|^2\left[J_0^2\left(\frac{kz\sigma_0^2\Delta}{4\sqrt{\varepsilon_2\mu-\sigma_0^2}}\right)J_0^2(k\sigma_0\rho)+\right.$$

$$\left.+4\cos^2(2\psi)J_1^2\left(\frac{kz\sigma_0^2\Delta}{4\sqrt{\varepsilon_2\mu-\sigma_0^2}}\right)J_2^2(k\sigma_0\rho)\right] \qquad (18)$$

From expression (18) we can see that the radial symmetry is broken, with rotation symmetry at an angle of 90 deg taking place. A similar result was obtained in [14] in the analysis of oblique incidence of the plane wave on a diffractive optical element (DOE) that forms Bessel beams in various diffraction orders.

The analysis of expression (18) shows that the most noticeable deviation from radial symmetry takes place in the absence of the first summand. This happens at distances corresponding to zeroes $j_{0,p}$ of the zero-order Bessel function $z_p = j_{0,p}4\sqrt{\varepsilon_2\mu-\sigma_0^2}\,/\,k\sigma_0^2\Delta$.

3. Numerical simulation

Let us carry out the numerical analysis of astigmatic transformation of Bessel beams in a lithium niobate crystal ($LiNbO_3$) with permittivities $\varepsilon_1 = 5.244$ and $\varepsilon_2 = 4.84$.

Two Bessel beams with different numerical apertures $\sigma_0 = 0.159$ and $\sigma_0 = 0.322$, with different polarization relative to the crystal axis were used for comparative modeling (see Fig. 1). The wavelength of laser radiation was $\lambda = 0.6328$ μm.

Table 1 shows the results of numerical simulation of the propagation of Bessel beams with different numerical apertures for various relative positions of the polarization plane and the crystal axis. The first column shows the central part of transverse distribution of the incident beam. In the second column the respective longitudinal intensity patterns are presented.

As can be seen from the results presented in Table 1 there is complete conformity of the numerical results to the analytical calculations given in the previous section. It is obvious that the Bessel beam propagates in the way it would propagate in an isotropic medium if its polarization is perpendicular to the crystal *c*-axis. In case of parallel polarization, the astigmatic transformation of the beam takes place, and the increase of the numerical aperture of the beam incident on the crystal increases the degree of astigmatism. Astigmatism also increases with the increase of the distance the beam travels in the crystal.

Figure 2 shows the distribution of intensity along the optical axis for various beam polarizations. Periodic changes of intensity in case of polarization parallel to the crystal *c*-axis can well be seen in this representation.

T a b l e 1. The results of numerical simulation for various relative positions of the polarization plane and the crystal axis (negative images).

The incident beam	Longitudinal intensity patterns z = [0, 1.05 mm] for various polarization of the incident beam
$\sigma_0 = 0.159$ 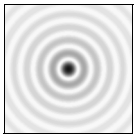	The polarization plane is parallel to the *c*-axis 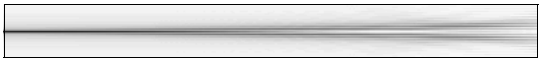
	The polarization plane is perpendicular to the *c*-axis 
$\sigma_0 = 0.322$ 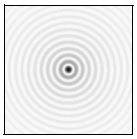	The polarization plane is parallel to the *c*-axis 
	The polarization plane is perpendicular to the *c*-axis 

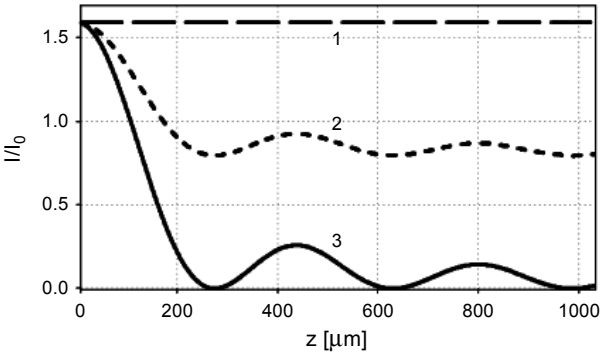

Fig. 2. The distribution of intensity along the optical axis for various beam polarizations ($\sigma_0 = 0.322$): *x*-polarized (parallel to the *c*-axis, curve 1), *xy*-polarized (at 45° to the *c*-axis, curve 2), *y*-polarized (perpendicular to the *c*-axis, curve 3).

The results of more detailed analysis of Bessel beam propagation $\sigma_0 = 0.322$ for various relative positions of the polarization plane and the crystal *c*-axis are presented in Figs. 3–5. The azimuth angle of the plane of polarization is denoted as φ_p, the azimuth angle of the crystal is denoted as φ_c. The figures show the intensities of *x*- and *y*-components of the field as well as the total intensity. To determine the components' distribution, a polarization analyzer can be used. The azimuth angle of the analyzer is denoted as φ_a.

It can be seen from Figs. 3–5 that astigmatic transformation has an impact only on the component parallel to the crystal *c*-axis while the perpendicular component passes the crystal like an isotropic medium. It should be noted that the intensity of the *y*-com-

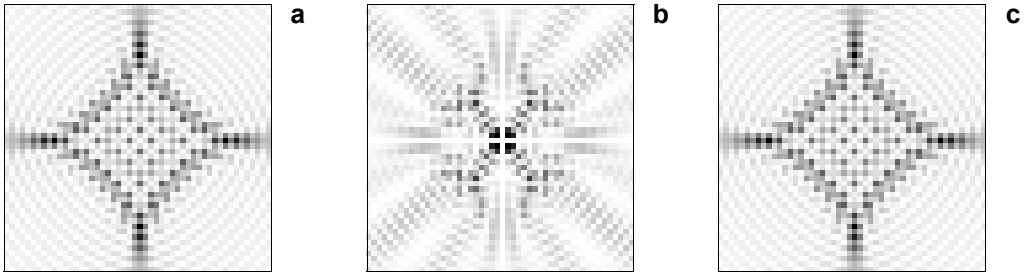

Fig. 3. Calculated intensity distributions (negative images) when the polarization is parallel to the *c*-axis ($\varphi_p = \varphi_c = 0°$): *x*-component ($\varphi_a = 0°$) – **a**, *y*-component ($\varphi_a = 90°$) – **b**, and total intensity – **c**.

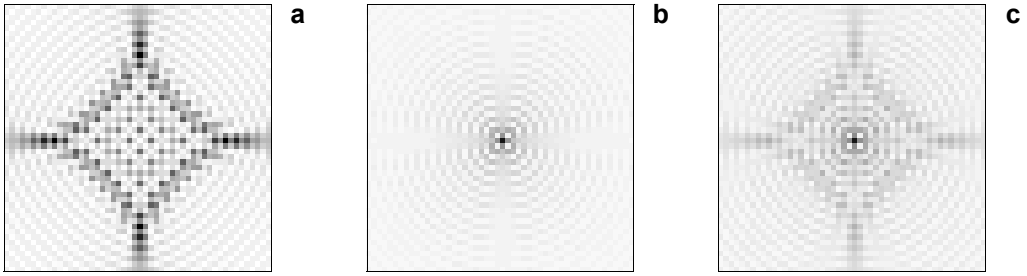

Fig. 4. Calculated intensity distributions (negative images) when the polarization is at 45° to the *c*-axis ($\varphi_p = 45°$, $\varphi_c = 0°$): *x*-component ($\varphi_a = 0°$) – **a**, *y*-component ($\varphi_a = 90°$) – **b**, and total intensity – **c**.

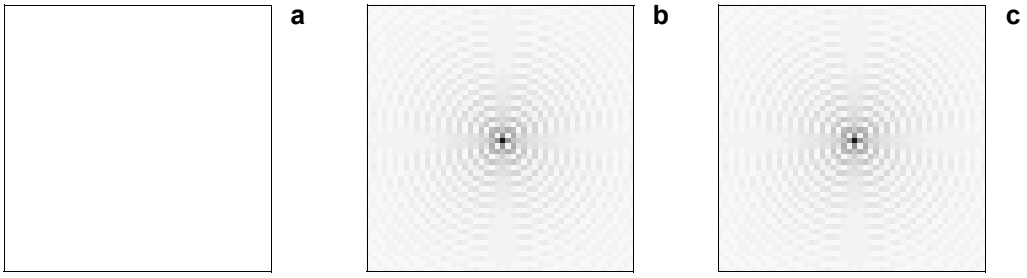

Fig. 5. Calculated intensity distributions (negative images) when the polarization is perpendicular to the *c*-axis ($\varphi_p = 90°$, $\varphi_c = 0°$): *x*-component ($\varphi_a = 0°$) – **a**, *y*-component ($\varphi_a = 90°$) – **b**, and total intensity – **c**.

ponent given in Fig. 3**b** is rather low, which is confirmed by the form of total intensity. Polarization diagonal to the crystal axis makes it possible to get a pattern that represents a visibly perceptible sum of intensities of the field orthogonal components.

4. Experimental analysis

To analyze the transformation of a zero-order Bessel beam in the $LiNbO_3$ *x*-cut, an optical setup was assembled shown in Fig. 6.

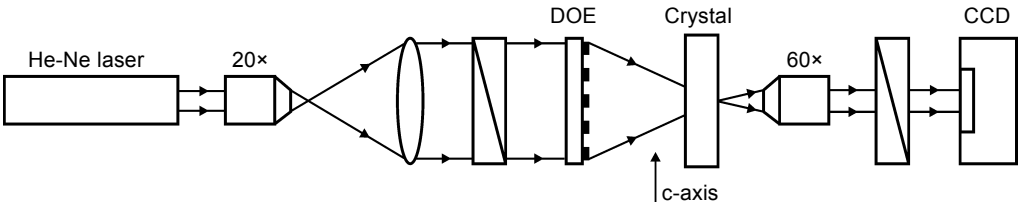

Fig. 6. The optical setup for experiments.

In order to form zero-order Bessel beams, an amplitude diffraction axicon was used with the diameter of 40 mm and ring period of $d = 2$ μm. The numerical aperture of such an axicon at the wavelength used $\lambda = 0.6328$ μm corresponds to $\sigma_0 = 0.322$. The amplitude mask of the axicon was produced on the CLWS-200 setup using the method of thermochemical oxidation of chrome 100 nm thick previously deposited on a quartz substrate with subsequent chemical removal of unmasked portions. The vector mode was used in recording, which made it possible to obtain a smooth boundary of topological elements.

A helium-neon laser LGN-207A was used as the source of radiation. The laser beam was expanded with a 20×-objective and a plane-convex lens with the diameter of 20 mm and focusing distance of 150 mm. Polarization of radiation was provided by a Glan–Taylor prism with the polarization coefficient not less than 5×10^5. The *x*-cut of congruent lithium niobate ($LiNbO_3$) 1050 ± 2 μm thick was used as a uniaxial crystal. The direction of the crystal *c*-axis was marked with facets, which made it possible to set the polarization plane of incident radiation at the required azimuth angle φ_c to the *c*-axis. The beam dimensions at the output of the crystal were increased by using a 60×-objective with a numerical aperture NA = 0.85, which exceeds the aperture of the axicon. A film polaroid of optical quality with the numerical aperture NA = 0.5 and a polarization coefficient not less than 10^4 served as an analyzer. The distribution of output beam intensity was recorded by a DCM 310 video camera with the resolution of 3 megapixels and 8-bit digit capacity of an analog-to-digital converter.

Figures 7–9 present the experimental results of Bessel beam transformation observed at the output of the *x*-cut of a $LiNbO_3$ crystal for various azimuth angles of

Fig. 7. Experimental intensity distributions when the polarization is parallel to the *c*-axis ($\varphi_p = \varphi_c = 0°$): *x*-component ($\varphi_a = 0°$) – **a**, *y*-component ($\varphi_a = 90°$) – **b**, and *x*- and *y*-component ($\varphi_a = 45°$) – **c**.

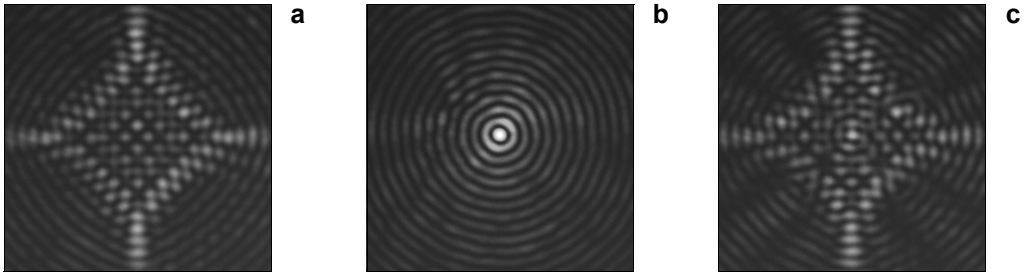

Fig. 8. Experimental intensity distributions when the polarization is at 45° to the *c*-axis ($\varphi_p = 45°$, $\varphi_c = 0°$): *x*-component ($\varphi_a = 0°$) – **a**, *y*-component ($\varphi_a = 90°$) – **b**, and *x*- and *y*-component ($\varphi_a = 45°$) – **c**.

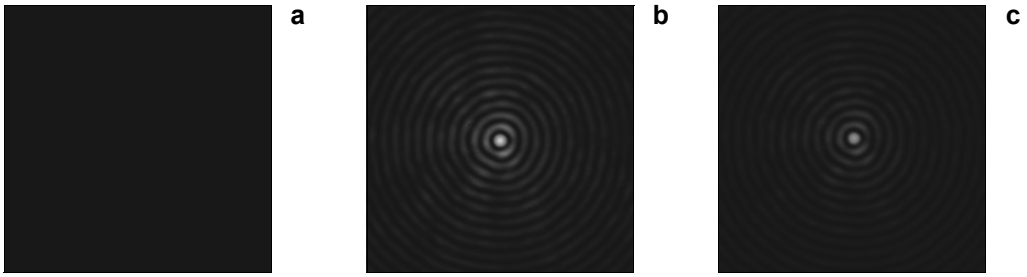

Fig. 9. Experimental intensity distributions when the polarization is perpendicular to the *c*-axis ($\varphi_p = 90°$, $\varphi_c = 0°$): *x*-component ($\varphi_a = 0°$) – **a**, *y*-component ($\varphi_a = 90°$) – **b**, and *x*- and *y*-component ($\varphi_a = 45°$) – **c**.

the polarizer φ_p, the optical axis of the crystal φ_c and the analyzer φ_a. The beam intensities on some fragments of the pictures differ since the emission power changes as the polarizer turns.

Experimental results are in a very good agreement with the numerical simulation and analytical calculations presented in previous sections.

5. Conclusions

We have analyzed zero-order Bessel beams propagation in lithium niobate crystal. The developed mathematical model and realized software make it possible to carry out detailed analysis of laser beam transformation in uniaxial crystals.

It is shown analytically that the transformation the Bessel beams undergo in an anisotropic crystal when they propagate perpendicular to the crystal *c*-axis is astigmatic and similar to the distortion in case of oblique incidence of the plane wave on the axicon or in the case of using a cylindrical lens. Variation of transverse intensity distribution is related to the extraordinary beam and consists in the transformation of the central ring into a set of point maxima. As it happens, the ring adjacent to the central area of the beam is subject to astigmatic skew distortions.

The implemented intensity distributions may have different numbers of point interference maxima in the plane of observation. Their number is determined by the numerical aperture and wavelength of the incident beam, crystal refraction index and thickness.

The obtained analytical expressions make it possible to establish conclusively the causes of breaking the beam radial symmetry in uniaxial crystals and to determine the crystal thickness that provides maximum efficiency of transformation. They will also be useful for rapid analysis of astigmatic transformation of laser beams in non-polar cuts of uniaxial crystals. It is possible to carry out contactless optical measurement of the thickness of anisotropic crystals by the form and distribution of output intensity.

Acknowledgements – The work was financially supported by the Russian Foundation for Basic Research (RFBR grants ## 13-07-00266 and 14-29-07133) and by the Ministry of Education and Science of the Russian Federation.

References

[1] KHILO N.A., PETROVA E.S., RYZHEVICH A.A., *Transformation of the order of Bessel beams in uniaxial crystals*, Quantum Electronics **31**(1), 2001, pp. 85–89.

[2] HACYAN S., JÁUREGUI R., *Evolution of optical phase and polarization vortices in birefringent media*, Journal of Optics A: Pure and Applied Optics **11**(8), 2009, article 085204.

[3] ZUSIN D.H., MAKSIMENKA R., FILIPPOV V.V., CHULKOV R.V., PERDRIX M., GOBERT O., GRABTCHIKOV A.S., *Bessel beam transformation by anisotropic crystals*, Journal of the Optical Society of America A **27**(8), 2010, pp. 1828–1833.

[4] KHILO N.A., *Diffraction and order conversion of Bessel beams in uniaxial crystals*, Optics Communications **285**(5), 2012, pp. 503–509.

[5] KHONINA S.N., MOROZOV A.A., KARPEEV S.V., *Effective transformation of a zero-order Bessel beam into a second-order vortex beam using an uniaxial crystal*, Laser Physics **24**(5), 2014, article 056101.

[6] LOUSSERT C., BRASSELET E., *Efficient scalar and vectorial singular beam shaping using homogeneous anisotropic media*, Optics Letters **35**(1), 2010, pp. 7–9.

[7] KHONINA S.N., KHARITONOV S.I., *Comparative investigation of nonparaxial mode propagation along the axis of uniaxial crystal*, Journal of Modern Optics **62**(2), 2015, pp. 125–134.

[8] KHONINA S.N., KARPEEV S.V., ALFEROV S.V., SOIFER V.A., *Generation of cylindrical vector beams of high orders using uniaxial crystals*, Journal of Optics **17**(6), 2015, article 065001.

[9] CIATTONI A., PALMA C., *Nondiffracting beams in uniaxial media propagating orthogonally to the optical axis*, Optics Communications **224**(4–6), 2003, pp. 175–183.

[10] DAJUN LIU, ZHONGXIANG ZHOU, *Various dark hollow beams propagating in uniaxial crystals orthogonal to the optical axis*, Journal of Optics A: Pure and Applied Optics **10**(9), 2008, article 095005.

[11] CHENGLIANG ZHAO, YANGJIAN CAI, *Paraxial propagation of Lorentz and Lorentz–Gauss beams in uniaxial crystals orthogonal to the optical axis*, Journal of Modern Optics **57**(5), 2010, pp. 375–384.

[12] GUOQUAN ZHOU, RUIPIN CHEN, XIUXIANG CHU, *Propagation of Airy beams in uniaxial crystals orthogonal to the optical axis*, Optics Express **20**(3), 2012, pp. 2196–2205.

[13] ZHAO BIN, LI ZHU, *Diffraction property of an axicon in oblique illumination*, Applied Optics **37**(13), 1998, pp. 2563–2568.

[14] KHONINA S.N., KOTLYAR V.V., SOIFER V.A., JEFIMOVS K., PÄÄKKÖNEN P., TURUNEN J., *Astigmatic Bessel laser beams*, Journal of Modern Optics **51**(5), 2004, pp. 677–686.

[15] BURVALL A., KOŁACZ K., GONCHAROV A.V., JAROSZEWICZ Z., DAINTY C., *Lens axicons in oblique illumination*, Applied Optics **46**(3), 2007, pp. 312–318.

[16] BENDERSKY A., PEREZ QUINTIAN F., REBOLLO M.A., *Modification of the structure of Bessel beams under oblique incidence*, Journal of Modern Optics **55**(15), 2008, pp. 2449–2456.
[17] ANGUIANO-MORALES M., *Transformation of Bessel beams by means of a cylindrical lens*, Applied Optics **48**(25), 2009, pp. 4826–4831.
[18] MANSURIPUR M., *Certain computational aspects of vector diffraction problems*, Journal of the Optical Society of America A **6**(6), 1989, pp. 786–805.
[19] KHONINA S.N., USTINOV A.V., KOVALYOV A.A., VOLOTOVSKY S.G., *Near-field propagation of vortex beams: models and computation algorithms*, Optical Memory and Neural Networks **23**(2), 2014, pp. 50–73.
[20] KHONINA S.N., KHARITONOV S.I., *An analog of the Rayleigh–Sommerfeld integral for anisotropic and gyrotropic media*, Journal of Modern Optics **60**(10), 2013, pp. 814–822.
[21] BATEMAN H., ERDELYI A., *Higher Transcendental Functions*, Vol. 1, McGraw-Hill, New York, 1953.
[22] PRUDNIKOV A.P., BRYCHKOV Y.A., MARICHEV O.I., *Integrals and Series: Elementary Functions*, Vol. 1, Nauka Publisher, Moscow, 1983 (in Russian).

Received August 8, 2015